Facile Interfacial Coprecipitation To Fabricate Hydrophilic Amine-Capped Magnetite Nanoparticles

Ke Tao, Hongjing Dou, and Kang Sun*

The State Key Lab of Metal Matrix Composites, Shanghai Jiao Tong University, Shanghai 200030, People's Republic of China

Received June 17, 2006. Revised Manuscript Received August 20, 2006

By using an interfacial coprecipitation method, hydrophilic magnetite nanoparticles capped with amine groups are facilely fabricated in this paper. In the approach, di-*n*-propylamine and a water/cyclohexane mixture act as the alkali and medium, respectively, so that the coprecipitate reaction is confined only to the interface between water and cyclohexane. The resultant nanoparticles are characterized by transmission electron microscopy (TEM), X-ray photoelectron spectroscopy (XPS), Fourier transform infrared (FTIR) spectroscopy, total nitrogen mass analysis, differential scanning calorimetry (DSC), and so forth. It is confirmed that the resultant nanoparticles possess not only relatively narrow size distribution but also a hydrophilic amine-decorated surface, which provides them with the capability of being further modified. Besides, the mechanism of the nucleation and growth of nanoparticles during interfacial coprecipitation is also discussed.

Introduction

Magnetic nanoparticles, especially magnetite (Fe_3O_4), have been intensively studied not only for fundamental scientific interest but also for their potential applications in magnetic recording media,[1] sensors,[2] catalysts,[3] and especially biomedical fields.[4−7] For all applications, facile and robust synthetic techniques are pursued. Among the synthetic methods of iron oxide nanoparticles, the one which is based on the decomposition of organic iron precusors, such as $Fe(C_6H_5N(NO)O^-)_3$,[8] $Fe(CO)_5$,[9] $Fe(acac)_3$ (acac: acetylacetonate),[10] was mostly of concern in recent years.[11] By this approach, the speed of nucleation and growth of nanocrystals are controlled by accurately adjusting the temperature and using abundant surfactants. Therefore, it is feasible to produce magnetic nanoparticles with controllable size, narrow size distribution, and generally a hydrophobic surface. Until now, the precursor decomposition approach has been investigated in many aspects, such as the elucidation of the mechanism,[12−14] the accurate control of the size[15] and the shape[16] of the nanoparticles, and even the selection of more economic precursors.[17] Undoubtedly, this method is a nearly perfect way to prepare monodispersed nanoparticles in the laboratory. However, the strict requirement of temperature controlling would be the bottleneck of applying this approach to industrial fabrication, and the resultant hydrophobic surface to some extent limits their use in biomedical fields.

Another chemical strategy to prepare iron oxide nanoparticles is based on the coprecipitation of Fe^{2+} and Fe^{3+} ions in a basic aqueous medium[18,19] or in a microemulsion system.[20,21] The great potential of this approach in making nanoparticles suitable for bioprocesses has been indicated in many references[22,23] because of the compatibility of the aqueous medium with biosystems. However, in the classical coprecipitation method, the size and size distribution of iron oxide nanoparticles are hard to control because the unlimited growth of the nanoparticles after nucleation cannot be prevented in a homogeneous aqueous medium. Besides, by this approach, carefully adjusting the pH value of the medium

* To whom correspondence should be addressed. Tel.: 86-21-62932555. Fax: 86-21-62830735. E-mail: ksun@sjtu.edu.cn.

(1) Sun, S. H.; Murray, C. B.; Weller, D.; Folks, L.; Moser, A. *Science* **2000**, *287*, 1989.
(2) Zeng, H.; Li, J.; Wang, Z. L.; Liu, J. P.; Sun, S. *Nature* **2002**, *420*, 395.
(3) Benz, M.; Van der Kraan, A. M.; Prins, R. J. *Appl. Catal., A* **1998**, *172*, 149.
(4) Häfeli, U.; Schütt, W.; Teller, J.; Zborowski, M. *Scientific and Clinical Applications of Magnetic Carriers*; Plenum Press: New York, 1997.
(5) Gu, H.; Xu, K.; Xu, C.; Xu, B. *Chem. Commun.* **2006**, 941.
(6) Mornet, S.; Vasseur, S.; Grasset, F.; Duguet, E. *J. Mater. Chem.* **2004**, *14*, 2161.
(7) Choi, J. W.; Ahn, C. H.; Bhansali, S.; Henderson, H. T. *Sens. Actuators, B* **2000**, *68*, 34.
(8) Rockenberger, J.; Scher, E. C.; Alivisatos, A. P. *J. Am. Chem. Soc.* **1999**, *121*, 11595.
(9) Hyeon, T.; Lee, S. S.; Park, J.; Chung, Y.; Na, H. B. *J. Am. Chem. Soc.* **2001**, *123*, 12798.
(10) Sun, S.; Zeng, H. *J. Am. Chem. Soc.* **2002**, *124*, 8204.
(11) Hyeon, T. *Chem. Commun.* **2003**, *9*, 927.
(12) Park, J.; An, K.; Hwang, Y.; Park, J. G.; Noh, H. J.; Kim, J. Y.; Park, J. H.; Hwang, N. M.; Hyeon, T. *Nat. Mater.* **2004**, *3*, 891.
(13) Yu, W. W.; Falkner, J. C.; Yavuz, C. T.; Colvin, V. L. *Chem. Commun.* **2004**, 2306.
(14) Casula, M. F.; Jun, Y.; Zaziski, D. J.; Chan, E. M.; Corrias, A.; Alivisatos, A. P. *J. Am. Chem. Soc.* **2006**, *128*, 1675.
(15) Park, J.; Lee, E.; Hwang, N. M.; Kang, M.; Kim, S. C.; Hwang, Y.; Park, J. G.; Noh, H. J.; Kim, J. Y.; Park, J. H.; Hyeon, T. *Angew. Chem., Int. Ed.* **2005**, *44*, 2872.
(16) Cheon, J.; Kang, N. J.; Lee, S. M.; Lee, J. H.; Yoon, J. H.; Oh, S. J. *J. Am. Chem. Soc.* **2004**, *126*, 1950.
(17) Jana, N. R.; Chen, Y.; Peng, X. *Chem. Mater.* **2004**, *16*, 3931.
(18) Kang, Y. S.; Risbud, S.; Rabolt, J. F.; Stroeve, P. *Chem. Mater.* **1996**, *8*, 2209.
(19) Freid, T.; Shemer, G.; Markovich, G. *Adv. Mater.* **2001**, *13*, 1158.
(20) Tartaj, P.; Serna, C. J. *Chem. Mater.* **2002**, *14*, 4396.
(21) Lee, Y.; Lee, J.; Bae, C. J.; Park, J. G.; Noh, H. J.; Park, J. H.; Hyeon T. *Adv. Funct. Mater.* **2005**, *15*, 503.
(22) Sahoo, Y.; Goodarzi, A.; Swihart, M. T.; Ohulchanskyy, T. Y.; Kaur, N.; Furlani, E. P.; Prasad, P. N. *J. Phys. Chem. B* **2005**, *109*, 3879.
(23) Cheng, F. Y.; Su, C. H.; Yang, Y. S.; Yeh, C. S.; Tsai, C. Y.; Wu, C. L.; Wu, M. T.; Shieh, D. B. *Biomaterials* **2005**, *26*, 729.

10.1021/cm0614113 CCC: $33.50
Published on Web 10/04/2006

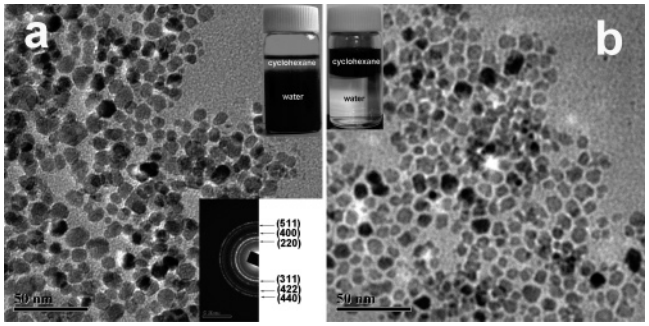

Figure 1. TEM images of S1a nanoparticles deposited from dispersion in water (a) and in cyclohexane after coating with oleic acid (b). Inset in the bottom of part a is the SAED of the S1a nanoparticles. Images represent S1a nanoparticles (in water) and oleic acid coated S1a nanoparticles (in cyclohexane) with the inset clearly showing particles transferred from water to nonpolar solvent after ligand exchange.

is inevitable to get nanosized magnetite particles, and stabilizing agents have to be added to keep the ferrofluid more stable.[24]

In the current work, we conduct coprecipitation of Fe^{2+} and Fe^{3+} on the interface of water/oil to fabricate Fe_3O_4 nanoparticles with nanoscaled size and unusual surface character. Compared with the existing approach, our approach offers a number of advantages. First, the di-*n*-propylamine which is almost insoluble in water is dissolved in cyclohexane to act as an OH^- precursor instead of a water-soluble alkali in classical coprecipitation so that the coprecipitation reaction was confined only proceeding on the water/cyclohexane interface and the unlimited growth of the Fe_3O_4 nucleus can be duly hindered. Second, the resultant nanoparticles possess an unusually hydrophilic surface which enables the nanoparticles to disperse in pure water stably. Third, the fabrication is convenient, and the hydrophilic nanoparticles could be obtained directly by only one step.

Experimental Section

Materials. $FeCl_2 \cdot 4H_2O$ (>98%), $FeCl_3 \cdot 6H_2O$ (>99%), cyclohexane (>99%), di-*n*-propylamine (>99%), oleic acid (>99%), and ethyl alcohol (>99%) were purchased from Sinopharm Chem Reagent Co. All these reagents were used without further purification. Milli-Q water was used in the synthesis.

Synthesis and Redispersion of Fe_3O_4 Nanoparticles. In a typical synthesis, 5 mmol of $FeCl_3 \cdot 6H_2O$ and 2.5 mmol of $FeCl_2 \cdot 4H_2O$ were dissolved in 100 mL of water; meanwhile, 5 mL of di-*n*-propylamine was diluted to 50 mL by cyclohexane. The aqueous solution of iron salt was added dropwise into the dipropylamine/cyclohexane solution under vigorous stirring (~1200 rpm) and supersonic dispersion (40 W supersonic power). The process of dropping was completed in about 15 min, and stirring was continued for another 15 min to complete the reaction. The synthesis was carried out at 25 °C under a nitrogen atmosphere. Thereafter, a bilayer liquid with a black Fe_3O_4/water subjacent layer and a colorless cyclohexane superstratum was obtained (as shown in the top inset of Figure 1a), indicating the hydrophilic surface of as-prepared nanoparticles. To purify the product, the subjacent Fe_3O_4 aqueous solution was rinsed with ethyl alcohol and centrifuged at 11 000 rpm for 10 min. This process was repeated five times, and then the Fe_3O_4 nanoparticles were collected by centrifugation and freeze-drying at −45 °C for 24 h. Other samples were prepared at various concentrations of iron salt. Besides, a contrast test was done by the similar process but without stirring and supersonication to investigate the influence of the water/cyclohexane interfacial area on the resultant nanoparticles. All samples synthesized by this interfacial coprecipitation are listed in Table 1. Another comparative sample (abbreviated as sample CP) was also prepared by a classical coprecipitate reaction (Massart's method).[25]

Table 1. Samples Produced by the Interfacial Coprecipitation Proposed in This Paper

samples	stirring or not	concentration of Fe^{3+} (mmol/L)[a]	concentration of di-*n*-propylamine (mL/L)[b]
S1a	yes	50	100
S2	yes	25	100
S3	yes	75	100
S1b	yes	50	200
S1c	yes	50	300
N1a	no	50	100

[a] $C_{Fe^{2+}} = C_{Fe^{3+}}/2$, C is concentration. [b] The concentration of di-*n*-propylamine in cyclohexane.

To prepare the nanoparticles coated with oleic acid, 200 mg of as-prepared nanoparticles and 0.2 mL of oleic acid were mixed with 100 mL of cyclohexane. The mixture was sonicated for 30 min and then centrifugated at 11 000 rpm for 10 min to get the Fe_3O_4 nanoparticles coated with oleic acid, which can be dispersed easily in a nonpolar solvent, such as cyclohexane (as shown in the inset in Figure 1b).

Characterization. For transmission electron microscopy (TEM) studies, the dispersions of nanoparticles in water or cyclohexane were drop-cast onto a carbon coated copper grid, and TEM images were taken on a JEOL JEM-2010 microscope at an accelerating voltage of 200 kV. To determine the size distribution and the mean average size, around 500 nanoparticles were measured for each sample. X-ray powder diffraction (XRD) patterns were measured in reflection mode (Cu Kα radiation) on a Bruker D8 diffractometer. X-ray photoelectron spectroscopy (XPS) spectra were recorded by using a Perkin-Elmer PHI5000c spectrometer with an Al Kα monochromatic X-ray source. Fourier transform infrared (FTIR) spectra were taken on a Bruker EQUINOX55 spectrometer. The sample was made by the pressed disc method after mixing dry nanoparticles with KBr. For measuring the content of nitrogen on the surface, 2.5 mmol of nanoparticles was dispersed in 1 L of water, and the mass of nitrogen was taken on a TOC/TN multi 3000 (ChD) analyzer (Analytik Jena, Germany). The number of ammonium molecules per nanoparticle (n) can be calculated based on $n = AM_{magnetite}/[(2.5 \times 10^{-3})M_{nitrogen}V\rho N_A]$, where A (ppm) is the value we got from the TOC/TN analyzer, M is the molecular weight, V (cm^3) is the volume of an individual nanoparticle, ρ (g/cm^3) is the density of bulk Fe_3O_4, and N_A is Avogadro's number. Differential scanning calorimetry (DSC) and thermogravimetric analysis (TGA) measurements were performed at a ramp rate of 10 °C/min under a nitrogen atmosphere using Q10 and TGA 2050 (TA Instruments), respectively. Magnetization measurements were performed on a vibrating sample magnetometer (VSM) at room temperature.

Results and Discussion

TEM observation of as-prepared nanoparticles S1a indicates that the nanoparticles possess a size of 10 ± 5 nm and a slightly irregular spherical shape (Figure 1a). The bottom inset in Figure 1a shows the selected area electron diffraction

(24) Sun, S.; Zeng, H.; Robinson, D. B.; Raoux, S; Rice, P. M.; Wang, S. X.; Li, G. *J. Am. Chem. Soc.*, **2004**, *126*, 273.

(25) Massart, R. *IEEE Trans. Magn.* **1981**, *MAG-17*, 1247.

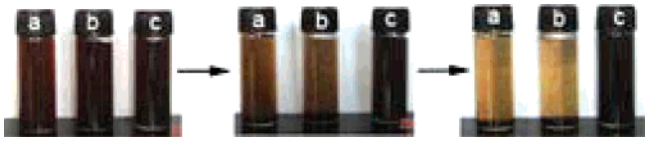

Figure 2. Photographs of aqueous suspensions of Fe_3O_4 nanoparticles prepared by classical coprecipitation (samples a and b in the figure were prepared at room temperature and 80 °C, respectively, according to ref 22 except that no stabilizing agent was added) and our method (c, sample S1a). Left image shows the suspensions immediately after preparation, center image was taken after about 7 min, and the photograph taken after about 15 min is shown at the right.

(SAED) pattern of as-prepared nanoparticles. Six distinct diffraction rings and their calculated *d*-spacings match well to that of Fe_3O_4.[26] To explore the effect of the concentration of iron salt on the resultant nanoparticles, S2 and S3 were prepared at various concentrations of iron salt. It is found by TEM study that the size and size distribution of S2 and S3 nanoparticles are similar to those of S1, indicating that the concentration of iron salt has no obvious effect on the size of nanoparticles. The TEM observation of two samples (S1b and S1c) prepared at different concentrations of amine also suggests that further increasing the concentration of di-*n*-propylamine in cyclohexane from 100 mL/L to 300 mL/L almost has no effect on the size of the nanoparticles. However, it is found that a minimal concentration of 80 mL/L is necessary for preparing Fe_3O_4 nanoparticles in this proposed approach; otherwise, dark-red FeOOH instead of Fe_3O_4 nanoparticles would be obtained.[27] The nanoparticles synthesized by this approach are able to be kept stable for about 20 h in pure water without any pH adjustment or stabilizing agent, which is much longer than the stabilizing time of nanoparticles prepared by classical coprecipitation in the same medium. Figure 2 shows the dispersing solution of Fe_3O_4 nanoparticles prepared by different methods after a series of durations. It is obvious that in the classical coprecipitation method, if no stabilizing agent (surfactant, acidic solution) was added, the as-prepared aqueous suspension cannot be kept stable even for several minutes. In addition, in our case, if dry nanoparticles are treated by the dilute HCl solution (0.01 M) as reported in literature[18] (the ratio between nanoparticles and HCl solution is about 500 mg/100 mL), the stabilized time could be prolonged to at least 2 weeks.

Dried nanoparticles can be easily redispersed in nonpolar solvent by coating with oleic acid or another alkyl carboxylic acid, such as stearic acid or myristic acid, the resultant solutions with a maximum concentration of 1 g/mL can be kept stable for more than 2 weeks without any precipitate. By TEM observations, it is obvious that after oleic acid coating the nanoaprticles disperse more separately (Figure 1b) compared with the original S1a nanoparticles (Figure 1a), and the interval of adjacent nanoparticles is close to the length of the oleic acid molecule (~23 Å), which shows that oleic acid has a stable interaction with the nanoparticles.[28]

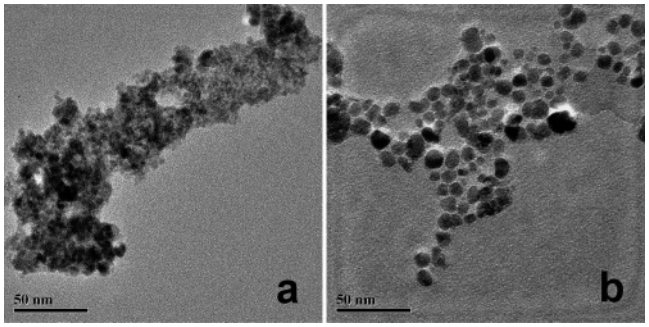

Figure 3. TEM images of sample N1a deposited from the dispersion in water (a) and oleic acid coated N1a deposited from the dispersion in cyclohexane (b).

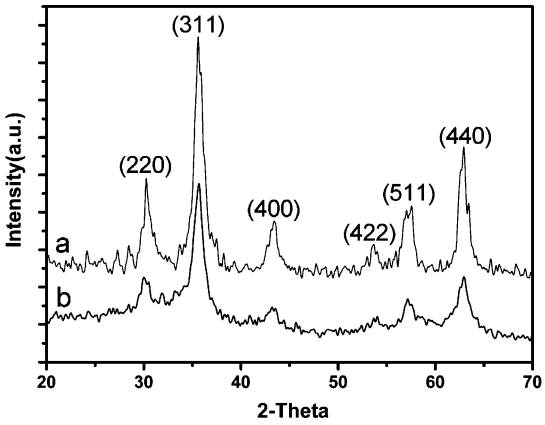

Figure 4. XRD patterns of S1a (a) and N1a (b)

In classical coprecipitation, adjusting the pH value of the aqueous solution is a key step to the formation and the stabilization of nanoparticles.[24] While in the approach proposed here, this adjustment can be omitted and there is only a minimum limit of the concentration of organic amine to get comparatively stable Fe_3O_4 nanoparticles. To explore the mechanism of the proposed approach, the synthesis was designed proceeding under the condition of no stirring. No nanoparticle but flocculent clusters can be observed in this sample (N1a) under TEM (Figure 3a). While it is interesting that, in TEM graphs of the same sample coated with oleic acid (Figure 3b), both nanoparticles and flocculent clusters can be found, the size distribution of these nanoparticles is obviously broader than that of sample S1a. In addition, it is worth pointing out that the N1a nanoparticles are able to disperse stably in pure water for at least 1 week, even longer than that of S1a. As we know, it is impossible to get Fe_3O_4 nanoparticles without stirring in classical coprecipitation, whereas in the present approach, the nanoparticles instead of macroscopical deposition can be obtained in a reaction medium without agitation, which provides powerful evidence that the coprecipitation proceed only on the interface of two phases.

The XRD patterns (Figure 4) of the sample S1a and N1a confirm the structure of the Fe_3O_4 nanocrystal because the position and relative intensity of the main peaks match well to those from the JCPDS card (19-0629) for Fe_3O_4.[29] The crystal domain size of the S1a Fe_3O_4 nanoparticles (Figure

(26) Cornell, R. M.; Schwertmann, U. *The Iron Oxides: Structure, Properties, Reactions, Occurences and Uses*, 2nd ed.; Wiley-VCH Verlag GmbH & Co. KGaA: Weinheim, 2003.
(27) Kim, D. K.; Mikhaylova, M.; Zhang, Y.; Muhammed, M. *Chem. Mater.* **2003**, *15*, 1617.
(28) Willis, A. L.; Turro, N. J.; O'Brien. S. *Chem. Mater.* **2005**, *17*, 5970.
(29) McClune, W. F. *Powder Diffraction File Alphabetical Index Inorganic Phase*; JCPDS: Swarthmore, 1980.

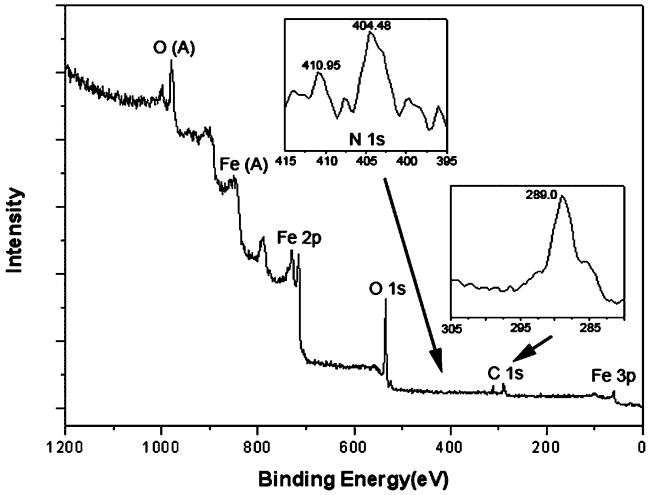

Figure 5. XPS spectra of sample S1a. The insets are expanded spectra of N 1s and C 1s.

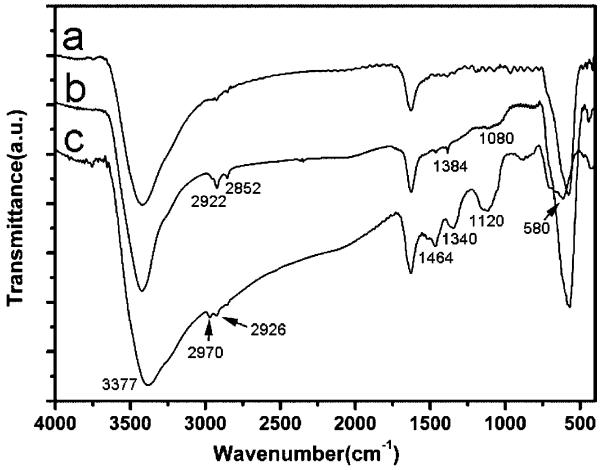

Figure 6. FTIR spectra of sample CP prepared by classical coprecipitation (a), S1a (b), and N1a (c).

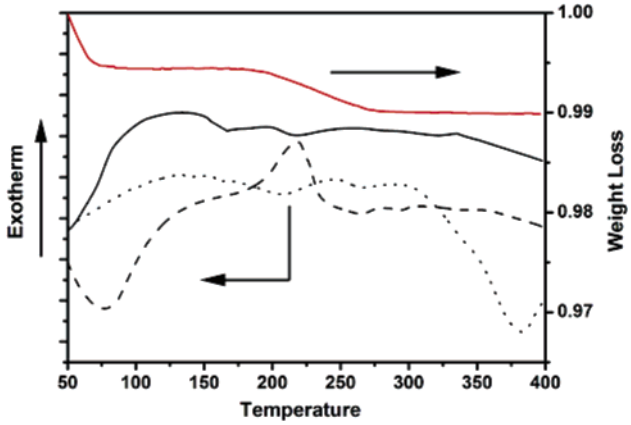

Figure 7. DSC curves for sample CP (solid line), S1a (dashed line), and oleic acid coated S1a (dotted line).

4a) is 10.8 nm calculated from peak broadening by using the Scherrer equation, which is in good agreement with the average diameter measured from TEM (about 10 nm) images. Although the composition of sample N1a can also be confirmed, the crystal domain size calculated from the Scherrer equation (9.8 nm) cannot match that observed in the TEM images, and the broadening of the XRD peaks is likely due to the low crystallinity of sample N1a.

XPS was used to explore the surface chemistry of the nanoparticles, by which the origin of their hydrophilic surface should be revealed. As shown in Figure 5, two peaks of Fe 2p and O 1s are typical for iron oxide, while the peaks ascribed to N 1s and C 1s indicate the existence of nitrogen on the surface of nanoparticles. Moreover, as shown in the insets of Figure 5, the shift and split of the N 1s peak and C 1s peak should be noticeable. The N 1s peak centered at 404.48 eV slightly shifts to a higher value compared with that of pure quaternary ammonium salt;[30] besides, a shakeup peak centered at 410.95 eV can also be observed. In view of the binding of ammonium salt on the surface of the nanoparticles, it can be proposed that the electrostatic interaction between the $R_2H_2N^+$ and $-O^{\delta-}-$Fe contributes to the higher binding energy of 404.48 eV and the shakeup peak at 410.95 eV for the amine adsorption mechanism.[23] The peak of C 1s is obviously composed of a main peak at 289.0 eV and two shoulder peaks at 292.6 and 285.2 eV. Among them, the shoulder peak at 285.2 eV should be ascribed to C in "CH_3-CH_2-", and two peaks at 289.0 and 292.6 eV are ascribed to the C connected with N and the C having interaction with O of iron oxide, respectively.[30] On the basis of the analysis of XPS results, it is obvious that a layer of ammonium salt was absorbed onto the surface of the Fe_3O_4 nanoparticles, and this resulted in the hydrophilicity of nanoparticles because of the existence of hydrophilic protonated amines.

To further confirm the existence of amines, another sample was prepared by classical coprecipitation as described in ref 25 (abbreviated as sample CP). Figure 6 shows the FTIR spectra of sample CP, S1a and N1a. In spectra b and c, the peaks around 2922 cm^{-1} and 2852 cm^{-1} assignable to asymmetric and symmetric vibration of C−H in $-CH_2-$ can be obviously found. The peak around 2970 cm^{-1} and 1384 cm^{-1} should be ascribed to the υ_{as} (asymmetrical stretching vibration) and δ_s (symmetrical deformation vibration) of C−H in $-CH_3$, respectively. Moreover, although the characteristic peaks of υ_{N-H} at about 3300 cm^{-1} (ref 31) were covered by the Fe_3O_4 peak from 3000−3750 cm^{-1}, a broadband from 1026 cm^{-1} to 1200 cm^{-1} attributed to the stretching peaks of C−N could confirm the presence of amine molecules. In spectrum c, the broadband at about 580 cm^{-1} corresponding to Fe−O vibrations is broader and weaker than that in spectrum b, which may be ascribed to the incomplete crystallization of sample N1a. In the spectrum of sample CP, these characteristic peaks of ammonium cannot be obviously found. By comparing FTIR spectra of S1a and N1a with that of CP, it is obvious there are amines existing on the nanoparticles synthesized by the proposed approach.

DSC thermograms of sample S1a before and after coating with oleic acid are shown in Figure 7. No obvious peaks can be found on the curve of sample CP; however, an

(30) Choudary, B. M.; Chowdari, N. S.; Madhi, S.; Kantam, M. L. *J. Org. Chem.* **2003**, *68*, 1736.

(31) Sadtler Research Laboratories. *Sadtler standard spectra: standard infrared grating spectra*; Sadtler Research Laboratories: Philadelphia, 1985.

Scheme 1. Schematic Illustration of the Interfacial Coprecipitation Synthesis to Magnetic Fe_3O_4 Nanoparticles

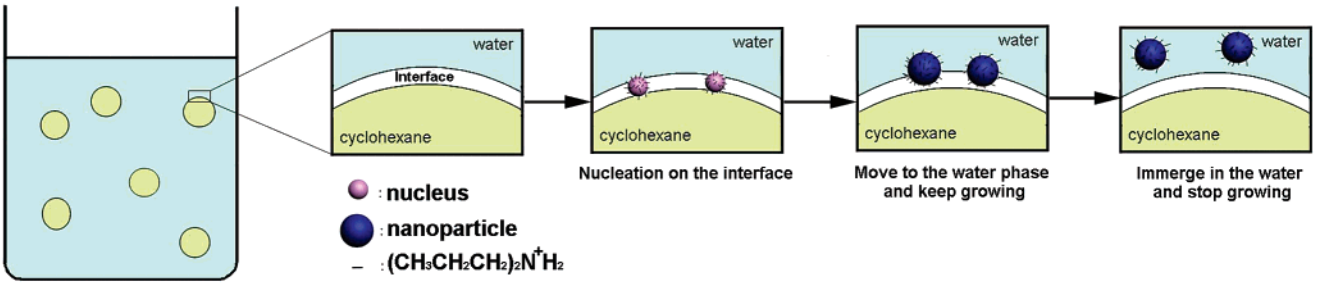

exothermic peak appears at about 223 °C on the curve of sample S1a (dash line). Besides, about 0.5% weight loss can be found around 223 °C (from 195 °C to 273 °C) on the TGA curves of S1a (red line in Figure 7), which may be ascribed to the decomposition or desorption of the absorbed ammonium salt. While on the curve of the oleic acid coated sample (dotted line), the exothermic peak at that temperature disappears and the endothermic peak assignable to oleic acid evaporating can be found at about 379 °C. Because the oleic acid molecules strongly anchored on the surface of Fe_3O_4 will evaporate at 378 °C,[32] we believe that there is relatively stable interaction between oleic acid and S1a nanoparticles.

The mass of the nitrogen element anchored on the nanoparticles was measured by a total nitrogen analyzer. The atomic ratio of Fe to N is determined to be 14 for sample S1a and 12 for sample N1a. This suggests that there are approximately 550 and 650 amine molecules on the surface of a 10 nm particle for S1a and N1a, respectively. This value is about one-fourth of the number of small molecules anchored on Fe_3O_4 nanoparticles by directly mixing particles and oleic acid[33] or by the hot decomposition method.[34] As referenced in many studies of the small molecule modified nanoparticle,[35] the one-step method described here could be used to make amine-capped nanoparticles which have the potential to be modified further by other active molecules.

The mechanism of the nucleation and growth of Fe_3O_4 nanocrystals in the proposed approach could be illustrated as Scheme 1. With the addition of the aqueous solution of iron salt into the organic phase, the two-phase mixture with an oil continuous phase and a water dispersed phase form because of their immiscibility, and di-*n*-propylamine molecules mainly locate on the interface of two phases because of the hydrophilicity of amine. Meanwhile, a burst of nucleation happens on the water/oil interface because there is the precursor of OH^- only near the interface. As a result of the reaction of iron salt and OH^-, the corresponding ionized di-*n*-propylamine molecules are anchored on the surface of the nucleus because of their interaction with OH^-. Thanks to the hydrophilicity of the ionized amine salt, the contact angle between the nucleus and water on the interface is less than 90°, and these nuclei would prefer to enter the water phase.[36] With the growth of the nucleus the nanocrystals immerge in the water phase completely. The absence of OH^- in the interior of the water phase make the further growth of these nancrystals impossible, and the existence of di-*n*-propylamine molecules on the periphery of nanocrystals prevent the agglomeration of these Fe_3O_4 nanocrystals. Moreover, because the thermal energy is comparable to the interfacial energy for nanoscale particles,[37] the spatial fluctuations may result in that the nanoparticles entered the water phase in different stages, resulting in a broadened size distribution of these nanoparticles. Surely, if stirring was carried out, the effect of the spatial fluctuation can be penetrated; thus, a relatively narrow distributed nanoparticles can be obtained under stirring compared with those without stirring. Considering the influence of various factors, such as oil phase, organic amine, and temperature, on the interface energy of two phases, the size and surface property of the resultant nanoparticles should be controllable by adjusting these factors.

According to LaMer's classical theory, the separation of nucleation and growth is necessary for the preparation of monodispersed nanoparticles.[38] As mentioned above, the separation of these two processes can hardly be controlled in the homogeneous solution by the classical coprecipitation method. In the microemulsion method, the growth is prevented by the limited size of the water pool, and in the organometallic precursor decomposition method, it is the mass of surfactant and fine control of temperature that hinder the growth and agglomeration of nanoparticles. Whereas in our approach the growth is stopped as soon as the nucleus enters a phase in which there is no adequate OH^-, this entering process is controlled by the surface nature of the nanoparticles, which provides a novel thinking about practising LaMer's theory in the fabrication of nanoparticles. Moreover, we believe that the reaction on various interfaces can be promisingly utilized for the synthesis of other kinds of nanoparticles, as indicated by the recent report.[39]

Magnetization curves of samples S1a and N1a measured by a VSM at 25 °C are shown in Figure 8. The saturation magnetization is found to be about 48 emu/g and 20 emu/g for S1a and N1a, respectively. The saturation magnetization of S1a is comparable to those surface modified Fe_3O_4 nanoparticles, whereas that of N1a is lower, which should be ascribed to the low crystallinity of this sample. The characteristic hysteresis loops of the ferrimagnetic substance

(32) Sahoo, Y.; Pizem, H.; Fried, T.; Golodnitsky, D.; Burstein, L; Sukenik, C. N.; Markovich, G. *Langmuir* **2001**, *17*, 7907.
(33) Shen, L.; Laibinis, P. E.; Hatton, T. A. *Langmuir* **1999**, *15*, 447.
(34) Li, Z.; Chen, H.; Bao, H.; Gao, M. *Chem. Mater.* **2004**, *16*, 1391.
(35) See, for example: Xu, C.; Xu, K.; Gu, H.; Zheng, R.; Liu, H.; Zhang, X.; Guo, Z.; Xu, B. *J. Am. Chem. Soc.* **2004**, *126*, 9938.
(36) Aveyard, R.; Binks, B. P.; Clint, J. H. *Adv. Colloid Interface Sci.* **2003**, *100−102*, 503.
(37) Duan, H.; Wang, D.; Kurth, D. G.; Möhwald, H. *Angew. Chem., Int. Ed.* **2004**, *43*, 5639.
(38) LaMer, V. K.; Dinegar, R. H. *J. Am. Chem. Soc.* **1950**, *72*, 4847.
(39) Wang, X.; Zhuang, J.; Peng, Q.; Li, Y. *Nature* **2005**, *437*, 121.

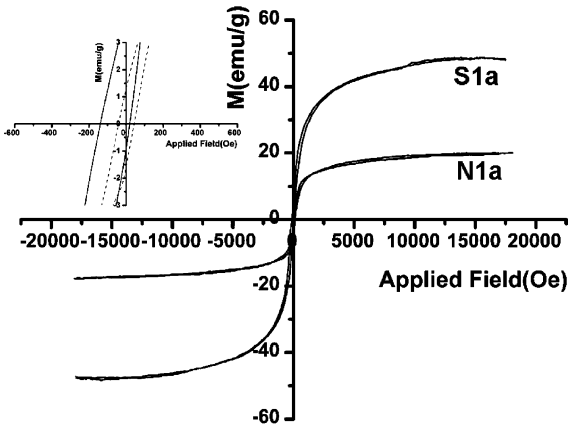

Figure 8. Room-temperature magnetization curves of samples S1a and N1a. Inset shows the expanded view of the low-field region of M−H loops: solid line, S1a, and dashed line, N1a.

are clearly observed in the magnifying figure of the center of the magnetization curve (as shown in the insets of Figure 8). It is worth noting that the hysteresis loop of sample S1a is not symmetric and shifts to the negative direction slightly. We propose that it should be attributed to the exchange coupling[40] effect of Fe_2O_3 which is slightly oxidized from Fe_3O_4 or amine absorbed on the surface of the nanoparticles with the inner ferrimagnetic Fe_3O_4.[41] Besides, the coercivity of S1a and N1a can be calculated from the half width of the hysteresis loops as about 80 and 45 Oe, respectively.

(40) O'Handley, R. C. *Modern Magnetic Materials Principle and Applications;* John Wiley & Sons, Inc.: Chichester, 2000.
(41) Meiklejohn, W. H.; Bean, C. P. *Phys. Rev.* **1956**, *102*, 1413.

Conclusion

In conclusion, we present a novel interfacial synthesis of magnetic nanoparticles with controllable size and surface property. This approach possesses advantages similar to those in classical coprecipitation but seems more convenient because the accurate adjustment of pH and agitation is not strictly required in the present approach. Besides, the coprecipitation reaction was confined by proceeding only on the water/cyclohexane interface so that Fe_3O_4 nanoparticles with relatively narrow size distribution and special surface property were obtained. The existence of amine on the periphery of the nanoparticles is certainly related to the origin of hydrophilicity and the stability of the nanoparticles and so far provides the possibility for further surface modification of nanoparticles. The driving force of the nucleus into the water phase caused by the amine decoration, which stops their further growth, is proposed as the key factor for the formation and stabilization of nanoparticles. In addition, there is relatively stable interaction between alkyl carboxylic acid and nanoparticles. Thus, oleic acid or other alkyl carboxylic acid can be easily coated on the nanoparticles to provide the solubility in nonpolar solvents.

Acknowledgment. This work was financially supported by Science and Technology Committee of Shanghai (Project No. 05ZR14084 and Project No. 04dz14002) and Young Scholar's foundation of Shanghai Jiao Tong Univ. We thank Instrumental Analysis Center of SJTU for the assistance with the measurements.

CM0614113